JOURNAL OF PROPULSION AND POWER
Vol. 19, No. 3, May–June 2003

Hysteresis Effects on Thrust Measurement and its Uncertainty

Joseph D. Sims*
NASA Marshall Space Flight Center, MSFC, Alabama 35812
and
Hugh W. Coleman†
University of Alabama in Huntsville, Huntsville, Alabama 35899

The work detailed herein describes a combination of experiments and numerical analysis meant to explore potential causes of both errors and hysteresis in a thrust measurement system and how they affect data reduction and uncertainty estimation. An uncertainty estimate of average hybrid motor thrust is also demonstrated. There were two major conclusions of this effort. First, hysteresis evident in a hybrid rocket motor test stand was eliminated through proper motor and thrust measurement system alignment. Second, Monte Carlo simulations showed that not including an elemental uncertainty contribution for hysteresis in an otherwise rigorous uncertainty propagation is a valid engineering approximation, when the experimental result is the average of data containing small (percentagewise) fluctuations.

Nomenclature

B_i	=	bias limit (systematic uncertainty)
B_{ik}	=	correlated bias limit
c	=	intercept of a first-order regression
h	=	trapezoidal rule integration constant
I_{sp}	=	sea-level specific impulse
I_{vac}	=	vacuum specific impulse
m	=	slope of a first-order regression
N	=	number of samples
n	=	number of subintervals used in a trapezoidal rule integration
P_i	=	precision limit (random uncertainty)
r	=	experimental result
$\bar{r}$	=	average of multiple experimental results
S_r	=	standard deviation of the mean of multiple results
$S_{regression}$	=	standard error of regression
T	=	instantaneous thrust
$\bar{T}$	=	average thrust
t	=	time
U_i	=	experimental uncertainty
X_i	=	primitive measured variable
Y_i	=	primitive measured variable
β	=	bias error
ε	=	precision error
θ_i	=	partial derivative of the result with respect to the ith primitive measurement
μ	=	parent population mean

Introduction

A FUNDAMENTAL question that arises in nearly all rocket engine testing is how well thrust can be measured. This question was raised during execution of the Hybrid Propulsion Demonstration Program (HPDP). A large portion of the HPDP work occurred at Test Stand 500 (TS 500) in the NASA Marshall Space Flight Center East Test Area. Specifically, the test position for the 24-in. hybrid motor includes a horizontal, single-axis thrust measurement capability of 50,000 lbf.

Historically, the stand had been plagued by hysteresis, so that a large body of data either suspected of, or known to, exhibit it was collected. Thus, parallel efforts aimed at 1) eliminating the presence of hysteresis altogether and 2) determining how to cope analytically with the historical data, were undertaken.

Motor Thrust Measurement System, 24-Inch

The thrust measurement system (TMS) at TS 500 has three elements common to most other TMSs.[1] First, it uses a fixed support structure against which the thrust load is reacted, namely the reaction structure, at left in Fig. 1. Second, it has a floating member (at right in Fig. 1) that transmits the thrust force to the reaction structure. Third, TS 500 has some nonideal behavior that influences the measurement such that the raw data need further reduction to provide the actual delivered thrust.

For this particular application, the reaction structure consists of two horizontal rectangular rails (Fig. 2) attached to a vertical, tubular-frame strongback that reacts against the thrust. Figure 2 also shows the knife edge on the right-hand rail that forces the motor carry carts (Fig. 3) to roll straight and true. Note that the carts provide for vertical and lateral adjustment of the motor.

To determine how the thrust stand and the test article interact, TS 500 uses a second load cell and a hydraulic cylinder (both of which are coaxial with the thrust measurement load cell). This arrangement, shown in Fig. 4, provides the working standard by which the thrust measurement load cell is calibrated. This is accomplished by actuating the hydraulic cylinder, which, by definition, imparts the standard input (the value read by the calibration load cell) to the thrust measurement load cell. Curve fitting this calibration data generates a correction curve used to reduce raw thrust data into delivered thrust data.[1]

As mentioned earlier, TS 500 has exhibited nonideal behavior. One example is the alternate load path resulting from the motor interfacing with the liquid oxygen (LOX) feed system[1,2] shown in Fig. 5. The effect of this load path is reduced by the flexure (highlighted in Fig. 5) but is not eliminated. This fact at TS 500 is one of the two primary reasons for performing the pretest calibration.

The primary nonideal behavior is hysteresis, evident in the calibration curve plotted in Fig. 6. Whether hysteresis itself increases the uncertainty of the hot-fire thrust measurement is addressed shortly, but, at the very least, hysteresis masks the ideal linear response. In fact, it is unclear whether the TMS responds linearly to the thrust generated during the motor firing or whether using a calibration curve that resembles Fig. 6 to reduce the raw thrust data is even meaningful.

Received 29 April 2002; revision received 15 December 2002; accepted for publication 23 January 2003.

*Liquid Propulsion Systems Engineer, Space Transportation Directorate, Combustion Devices and Turbomachinery. Member AIAA.

†Professor, Propulsion Research Center, Department of Mechanical and Aerospace Engineering. Associate Fellow AIAA.

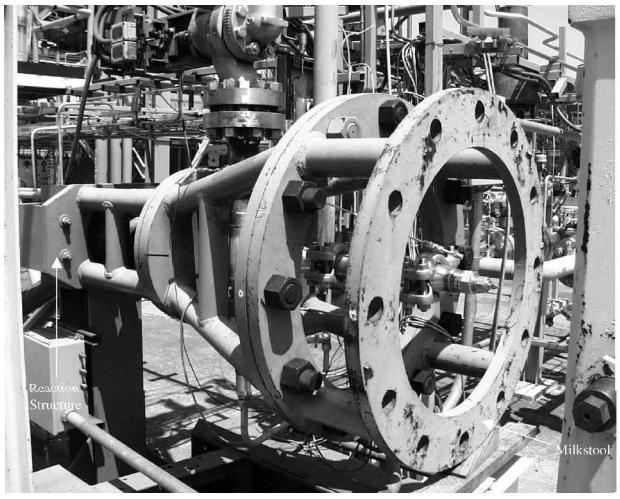

Fig. 1 Close-up of the 24-in. motor test stand.

Fig. 2 Thrust stand rails.

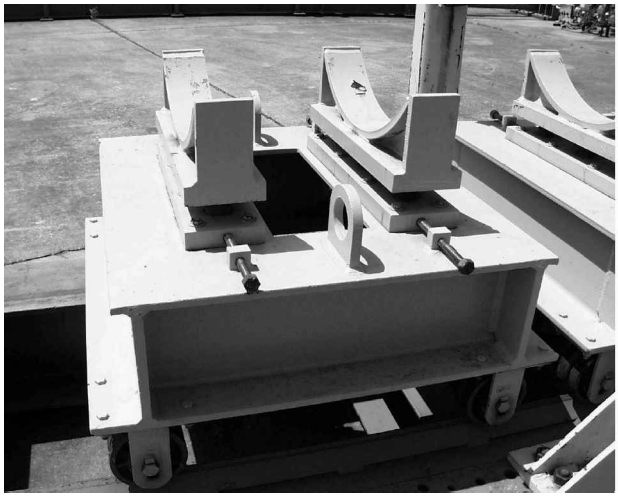

Fig. 3 Motor cart.

Experimental Study of Hysteresis

Members of the HPDP Consortium offered three possible causes of hysteresis. These opinions formed the basis for the experiments.

The first possibility was an issue of dynamics. Because the TMS is essentially a mass–spring–damper system, it was unclear how the loading rate would affect the calibration curve. An analysis suggested it could have a dramatic effect (R. McLeod, unpublished HPDP memorandum, April 1997). Even though test stand dynamic analysis indicated that its fundamental frequency should be ~25 Hz (HPDP Consortium members, private communications, April–May 1997) (a much greater frequency than that used in any calibration), this issue was addressed experimentally by simply doubling the loading rate and comparing it to the typical case.

Fig. 4 Calibration load cell and hydraulic cylinder.

Fig. 5 LOX feed system.

The second possibility was some unforeseen interaction with the LOX feed system, such as a broken or binding flexure. Although it was understood that this interplay between the feed system and the motor would affect the slope and offset of the calibration curve fit, it was not clear how much it would affect them or whether it would affect hysteresis. This was addressed by completing calibrations with the feed system in three different states 1) ambient temperature and ambient pressure, 2) cryogenic temperature and ambient pressure, and 3) cryogenic temperature and full test pressure (~1500 psig).

The third possibility was simply friction within the TMS itself. There was speculation that the rods that connect the milkstool to

the measurement system were binding in their sleeves and that the motor carts were somehow also involved. Therefore, first, the overall alignment of the stand itself was verified, and then a procedure to align the floating portion of the TMS and the motor properly was generated by trial and error.

Dynamics and Feed System Effects Results

Table 1 summarizes the conditions used in this first series of calibration tests. To discover any effects that might exist, the calibration data were fit with a first-order least-squares regression. Then, the maximum hysteresis deviation (the maximum difference between the regression and the raw calibration data) was calculated for each test and, for completeness, the slopes and intercepts of the six regressions were compared for differences.

Table 2 shows the results of the first six runs. Note that tests 1–4 were run before a different motor firing than tests 5 and 6, which explains the minor differences in slope and intercept values between replicated tests. As can be seen, every calibration showed similarly high hysteresis deviation, and every curve resembled that in Fig. 6. This implies that neither dynamics nor the state of the feed system contributes to hysteresis. On the other hand, note that the feed system state does affect the regression. On examination of Table 2, the data show a 1–2% difference in slope due to temperature and pressure effects. The intercept value also changes by nearly 19% from temperature effects. This implies that all calibration tests for actual motor firings should be run with the feed system in its expected test conditions.

Table 1 Calibration test conditions

Run	Feed system pressure	Feed system temperature	Loading ramp rate, lbf/s
1	Ambient	Ambient	1000
2	Ambient	Ambient	2000
3	Ambient	Cryogenic	1000
4	1500 psig	Cryogenic	1000
5	Ambient	Cryogenic	1000
6	1500 psig	Cryogenic	1000

Table 2 Initial calibration curve results

Run	Slope	Intercept, lbf	Maximum hysteresis, lbf
1	0.79	1763	1284
2	0.79	1749	1246
3	0.78	1404	1209
4	0.80	1442	1348
5	0.81	1490	1177
6	0.85	1272	1372

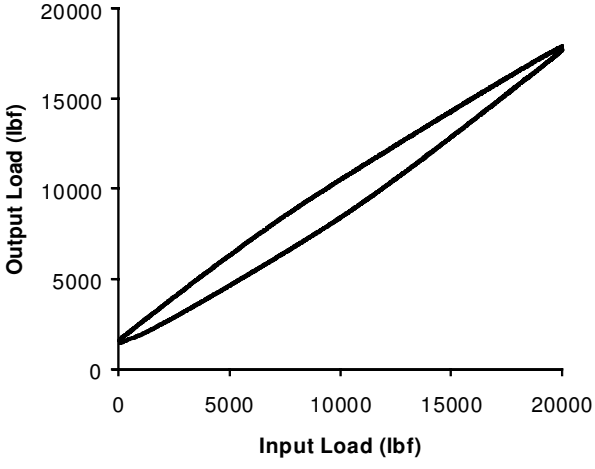

Fig. 6 Typical calibration curve from TS 500 that exhibits hysteresis.

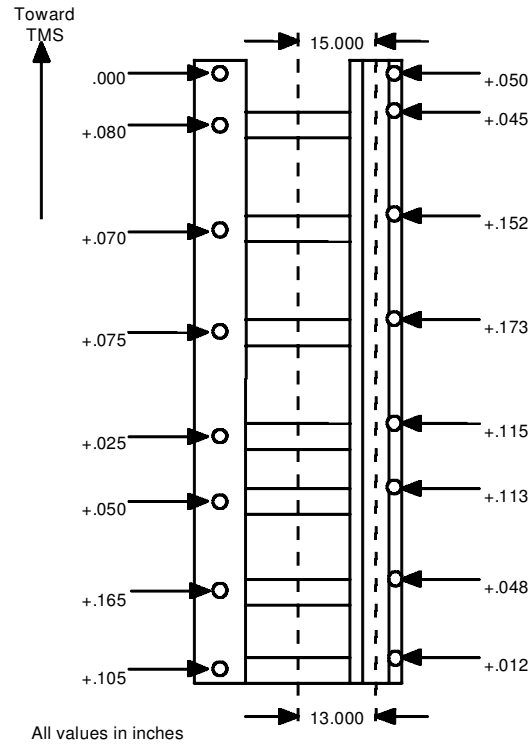

Fig. 7 Stand alignment results.

Friction Effects Results

The first operation was to verify the as-built condition of the thrust stand to see whether any misalignments existed that might create sliding friction in the floating portion of the TMS. The data shown in Fig. 7 were generated by the use of optical theodolites. The arrows, pointing to the circles represent the elevation difference (in inches) between that particular point and the reference elevation at the upper-left corner of the stand. The data show that the horizontal rails are not perfectly level, though they were installed on concrete not specifically leveled for this purpose. Additionally, there is measurable runout fore to aft, as shown by the difference in centerline measurements (also in inches) at the top and bottom of Fig. 7. However, the motor and carts move less than 0.020 in. for a full thrust load, and so it was concluded that the stand was as square as it practically needed to be.

The next step was to align the motor coaxial to the thrust measurement load cell, not only following Interagency Chemical Rocket Propulsion Group (ICRPG) guidelines[3] to ensure accurate thrust measurement, but to try to isolate the source of the hysteresis. Historically, motor alignment was assumed good simply by placing the carts properly on the rails and the knife edge, placing the motor in the carts and then bolting the head end to the milkstool. This time, however, once the motor was in place and connected to the milkstool, the motor was adjusted coaxial to the thrust load cell (to within 0.050 in. in both pitch and yaw) using the theodolites to gauge the movement. Figure 8 shows the results for test 7. The absolute value of the hysteresis deviation was as bad as any previous attempt, but the shape of the curve is quite different. The two knees were felt to be effects of the alignment, just not those intended.

Because the motor was attached to the milkstool before being aligned, the implicit assumption was that the milkstool itself was already coaxial to the thrust measurement load cell and would stay aligned, regardless of the motor position. After measuring it, however, it was clear that the milkstool itself droops because it is cantilevered without any support underneath. It was also suspected that trying to align the motor while it was attached to the milkstool was forcing the milkstool even further out of alignment.

To test this hypothesis, the motor and the milkstool were independently aligned and connected once alignment was achieved. Because of difficulties with moving the milkstool and imperfections in the

Table 3 Final calibration curve results

Run	Slope	Intercept, lbf	Maximum hysteresis, lbf
7	0.85	1293	1253
8	0.97	200	156

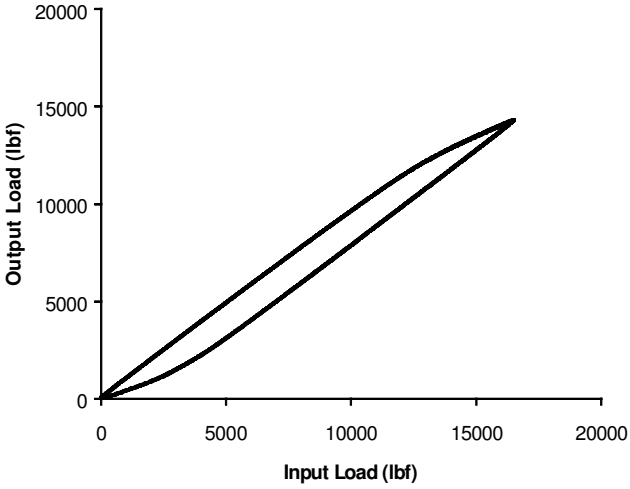

Fig. 8 Calibration curve after the first motor alignment (test 7).

Fig. 9 Calibration data after proper motor/TMS alignment (test 8).

assembly of the entire floating portion of the TMS, the milkstool was simply adjusted as close to coaxial as possible (~0.25 in.). However, both ends of the motor were less than 0.010 in. from perfect coaxial alignment. The feed system was then brought down to cryogenic temperatures and pressurized, and a series of ten loading cycles was completed. Figure 9 shows the results graphically, and Table 3 compares regression coefficients and hysteresis deviation between calibration 8 and the preceding one (7). The results clearly indicate that minimizing alignment errors minimizes hysteresis. The slight hysteresis that remains in this final calibration is likely due to the friction resulting from the inability to align the milkstool perfectly.

Analytical Study of Hysteresis

The method used to define how good thrust measurement is at TS 500 is detailed uncertainty analysis. Uncertainty analysis has been applied in a broad variety of situations, and it benefits experimentation in two ways. First, of course, it generates an estimate of the uncertainty in a given experimental result. As importantly, though, it allows one to learn which measurements contribute the most to the overall uncertainty, and hence, require the strictest experimental control.

Uncertainty Analysis[4,5]

The word "accuracy" is generally used to indicate the relative closeness between an experimentally determined value of a quantity and its true value. Error is the difference between the experimentally determined value and the truth; therefore, as error decreases, accuracy is said to increase. Only in rare instances is the true value of a quantity known. Thus, it is necessary to estimate error, and that estimate is called an uncertainty U. Uncertainty estimates are made at some confidence level. A 95% confidence estimate, for example, means that the true value of the quantity is expected to be within the $\pm U$ interval about the experimentally determined value 95 times out of 100.

Total error can be considered to be composed of two components: a precision (random) component ε and a bias (systematic) component β. An error is classified as precision if it contributes to the scatter of the data; otherwise, it is a bias error. As an estimator of β, a systematic uncertainty or bias limit B is defined. A 95% confidence estimate is interpreted as the experimenter being 95% confident that the true value of the bias error, if known, would fall within $\pm B$. A useful approach to estimating the magnitude of a bias error is to assume that the bias error for a given case is a single realization drawn from some statistical parent distribution of possible bias errors. As an estimator of the magnitude of the precision errors, a random uncertainty or precision limit P for a single reading is defined. A 95% confidence estimate of P is interpreted to mean that the $\pm P$ interval about the single reading of X_i should cover the (biased) parent population mean μ, 95 times out of 100. In nearly all experiments, the measured values of different variables are combined using a data reduction equation (DRE) to form some desired result. A general representation of a DRE is

$$r = r(X_1, X_2, \ldots, X_J) \tag{1}$$

where r is determined from J measured variables X_i. Each of the measured variables contains bias errors and precision errors. These errors in the measured values then propagate through the DRE, thereby generating the bias and precision errors in r.

If the "large sample assumption" is made,[4] then the 95% confidence expression for U_r becomes

$$U_r^2 = B_r^2 + P_r^2 \tag{2}$$

where the systematic uncertainty (bias limit) of the result is defined as

$$B_r^2 = \sum \theta_i^2 B_i^2 + 2 \sum_{i=1}^{J-1} \sum_{k=i+1}^{J} \theta_i \theta_k B_{ik} \tag{3}$$

and the random uncertainty (precision limit) of the result is defined as

$$P_r^2 = \sum_{i=1}^{J} \theta_i^2 P_i^2 \tag{4}$$

The bias limit estimate for each X_i variable is the root sum square combination of its elemental systematic uncertainties

$$B_i = \left[\sum_{j=1}^{M} (B_i)_j^2 \right]^{\frac{1}{2}} \tag{5}$$

and B_{ik} is the 95% confidence estimate of the covariance appropriate for the bias errors in X_i and the bias errors in X_k. It is determined from

$$B_{ik} = \sum_{\alpha=1}^{L} (B_i)_\alpha (B_k)_\alpha \tag{6}$$

where the measurements of variables X_i and X_k share L identical error sources. These terms account for correlation between bias errors in different measurements. The possibility of correlated random errors, which is unlikely, is not reflected in Eq. (13).

Additionally,

$$\theta_i = \frac{\partial r}{\partial X_i} \tag{7}$$

If multiple results taken at the same experimental setting are available, then P_r can be directly calculated instead of using the propagation equation (13). That 95% confidence random uncertainty can be estimated using

$$P_r = 2S_r \tag{8}$$

where S_r is the standard deviation of the sample population given by

$$S_r = \left[\frac{1}{N-1}\sum_{i=1}^{N}(r_i - \bar{r})^2\right]^{\frac{1}{2}} \tag{9}$$

and the mean value is defined as

$$\bar{r} = \frac{1}{N}\left[\sum_{i=1}^{N} r_i\right] \tag{10}$$

DRE Development

For the 24-in. hybrid motor, average thrust is calculated using the time integral:

$$\bar{T} = \frac{\int_{t_{\text{start}}}^{t_{\text{end}}} T_{\text{delivered}}\,\mathrm{d}t}{t_{\text{end}} - t_{\text{start}}} \tag{11}$$

The integral is numerically estimated using the trapezoidal rule[6]:

$$\int_{t_{\text{start}}}^{t_{\text{end}}} T_{\text{delivered}}\,\mathrm{d}t \approx h\left(\frac{1}{2}T_{t_{\text{start}}} + T_{t_{\text{start}+1}} + \cdots + T_{t_{\text{end}-1}} + \frac{1}{2}T_{t_{\text{end}}}\right) \tag{12}$$

where h is given by

$$h = (t_{\text{end}} - t_{\text{start}})/n \tag{13}$$

and n is the number of subintervals into which the domain is divided, that is, there are $n+1$ raw thrust data points.

Combining Eqs. (1–3) gives

$$\bar{T} = \frac{\left\{[(t_{\text{end}} - t_{\text{start}})/n] * \left(\frac{1}{2}T_{t_{\text{start}}} + T_{t_{\text{start}+1}} + \cdots + T_{t_{\text{end}-1}} + \frac{1}{2}T_{t_{\text{end}}}\right)\right\}}{t_{\text{end}} - t_{\text{start}}} \tag{14}$$

so that, through simplification, the DRE becomes

$$\bar{T} = \left[\frac{1}{2}T_{t_{\text{start}}} + \sum_{i=2}^{n} T_i + \frac{1}{2}T_{t_{\text{end}}}\right] \Big/ n \tag{15}$$

Because $T_{\text{delivered}}$, the actual delivered thrust, is found by correcting the raw thrust data using a regression of the prefire calibration data,[1] the following equation is also important:

$$T_{\text{delivered}} = mT_{\text{raw}} + c \tag{16}$$

The equations for the coefficients in a first-order, least-squares, linear regression are given hereafter:

$$m = \frac{N\sum_{i=1}^{N} X_iY_i - \sum_{i=1}^{N} X_i \sum_{i=1}^{N} Y_i}{N\sum_{i=1}^{N}\left(X_i^2\right) - \left(\sum_{i=1}^{N} X_i\right)^2} \tag{17}$$

$$c = \frac{\sum_{i=1}^{N}\left(X_i^2\right)\sum_{i=1}^{N} Y_i - \sum_{i=1}^{N} X_i \sum_{i=1}^{N}(X_iY_i)}{N\sum_{i=1}^{N}\left(X_i^2\right) - \left(\sum_{i=1}^{N} X_i\right)^2} \tag{18}$$

where N is the number of points in the calibration data used for the regression, the X_i are the input calibration loads measured with the calibration load cell, and the Y_i are the calibration output loads measured with the thrust measurement load cell.

Therefore, combining Eqs. (6–8) results in the overall DRE for average delivered thrust:

$$\bar{T} = \left\{\frac{1}{2}\left[m(X_i, Y_i)T_{\text{raw},t_{\text{start}}} + c(X_i, Y_i)\right] + \sum_{i=2}^{n}[m(X_i, Y_i)T_{\text{raw,i}} + c(X_i, Y_i)] + \frac{1}{2}\left[m(X_i, Y_i)T_{\text{raw},t_{\text{end}}} + c(X_i, Y_i)\right]\right\} \Big/ n \tag{19}$$

Monte Carlo Simulations

Because an uncertainty analysis results in an estimate of the experimental uncertainty, a term (or a number of terms) could be added to the propagation equation in an attempt to estimate the uncertainty associated with hysteresis. One could approximate that uncertainty by simply calculating the difference between the actual calibration data and the regression and treating it as a loss in resolution. At TS 500, this difference was normally ~1300 lbf, a prohibitively large magnitude that, if added to the uncertainty estimate for average thrust, would relegate most sets of historical data useless.

Alternatively, one could ignore its presence altogether by arguing that hysteresis was only seen when the motor and TMS were displaced slowly and over relatively large distances, that is, zero to full scale and back. Given the high-frequency, small-displacement oscillations that occur during steady motor operation, it seems reasonable to conclude that, even if hysteresis occurred, it would be much lower in magnitude than that seen in a calibration load cycle. This is because sliding friction causes hysteresis in the TMS, and so a smaller displacement will result in lower total friction effects. Furthermore, the typical calibration curve from TS 500 was symmetric, implying that, overall, the TMS response is well represented by a first-order linear regression. Thus, two Monte Carlo simulations were used to explore whether uncertainty estimates for the slope and intercept, resulting from a regression of data that contain hysteresis, are valid when no terms are propagated to account for the hysteresis.

In each iteration, the line

$$y = x \tag{20}$$

was first generated (that is, $m = 1.0$ and $c = 0.0$), which represents the true model of the TMS response. Next, the y values were perturbed using a quadratic function to apply hysteresis to the true values. Then, error terms (both systematic and random) of differing magnitudes were added to both x and y values (to generate the experimental result. Finally, the uncertainty estimate was calculated using the method of Brown et al.)[5] with no additional terms added to account for hysteresis. A counter was incremented if the $\pm U_{\text{slope}}$ interval around the experimental slope contained 1.0, and another one was incremented if the $\pm U_{\text{intercept}}$ interval around the experimental intercept contained 0.0. After 10,000 iterations, percent coverages for both results were calculated.

The general forms of the propagation equations for the uncertainties in slope and intercept, ignoring correlated random uncertainties, were used[5]:

$$U_m^2 = \sum_{i=1}^{N}\left(\frac{\partial m}{\partial X_i}\right)^2 P_{X_i}^2 + \sum_{i=1}^{N}\left(\frac{\partial m}{\partial Y_i}\right)^2 P_{Y_i}^2 + \sum_{i=1}^{N}\left(\frac{\partial m}{\partial X_i}\right)^2 B_{X_i}^2 + 2\sum_{i=1}^{N-1}\sum_{k=i}^{N}\left(\frac{\partial m}{\partial X_i}\right)\left(\frac{\partial m}{\partial X_k}\right)B_{X_iX_k} + \sum_{i=1}^{N}\left(\frac{\partial m}{\partial Y_i}\right)^2 B_{Y_i}^2 + 2\sum_{i=1}^{N-1}\sum_{k=i}^{N}\left(\frac{\partial m}{\partial Y_i}\right)\left(\frac{\partial m}{\partial Y_k}\right)B_{Y_iY_k} + 2\sum_{i=1}^{N}\sum_{k=i}^{N}\left(\frac{\partial m}{\partial X_i}\right)\left(\frac{\partial m}{\partial Y_k}\right)B_{X_iY_k} \tag{21}$$

$$U_c^2 = \sum_{i=1}^{N}\left(\frac{\partial c}{\partial X_i}\right)^2 P_{X_i}^2 + \sum_{i=1}^{N}\left(\frac{\partial c}{\partial Y_i}\right)^2 P_{Y_i}^2 + \sum_{i=1}^{N}\left(\frac{\partial c}{\partial X_i}\right)^2 B_{X_i}^2 + 2\sum_{i=1}^{N-1}\sum_{k=i}^{N}\left(\frac{\partial c}{\partial X_i}\right)\left(\frac{\partial c}{\partial X_k}\right) B_{X_i X_k} + \sum_{i=1}^{N}\left(\frac{\partial c}{\partial Y_i}\right)^2 B_{Y_i}^2 + 2\sum_{i=1}^{N-1}\sum_{k=i}^{N}\left(\frac{\partial c}{\partial Y_i}\right)\left(\frac{\partial c}{\partial Y_k}\right) B_{Y_i Y_k} + 2\sum_{i=1}^{N}\sum_{k=i}^{N}\left(\frac{\partial c}{\partial X_i}\right)\left(\frac{\partial c}{\partial Y_k}\right) B_{X_i Y_k} \tag{22}$$

Also, the amount of hysteresis was determined by multiplying the prescribed level (a percent of full scale) by the 20,000-unit full-scale reading. For example, if the hysteresis level was 10% of full scale (FS), the actual deltas applied to the true y values were determined by a quadratic function that passes through (0, 0) and (20,000; 20,000), with the maximum 2000-lbf hysteresis occurring at its inflection point.

The first simulation, intended to have a more generally applicable result, allowed precision and bias limits for x and y to vary independently. This simulates the common situation where x and y values are not gathered by the same instrument. Table 4 summarizes the settings for this first simulation.

The second simulation was designed to simulate instances where the x and y values came from similar instruments, as is the case with the TMS at TS 500. This assumption forces the normalized standard deviation of each type of error to be the same for the x and y values (though it does not necessarily mean the actual magnitude of the error is the same for both x and y). Furthermore, this gives rise to the possibility of correlated bias effects. Table 5 summarizes the settings for the second simulation.

Monte Carlo Simulation Results

Table 6 shows that the simulations substantiate the claim that the presence of hysteresis, in this instance, does not contribute to the uncertainty in slope and intercept. The average percent coverage in all four cases is essentially 95%, varying between 93 and 97%. Even these extreme values are acceptable because, in actual engineering applications, the experimentalist would be hard pressed to resolve a 93%-confident uncertainty estimate from a 95%-confident uncertainty estimate.

Table 4 Factors and levels for simulation 1

Factor	Low level, % FS	High level, % FS
x precision limit	0.25	2.0
y precision limit	0.25	2.0
x bias limit	0.25	2.0
y bias limit	0.25	2.0
Hysteresis	1.0	10.0

Table 5 Factors and levels for simulation 2

Factor	Low level, % FS	High level, % FS
Precision limit	0.25	5.0
Bias limit	0.25	5.0
Hysteresis	5.0	20.0

Table 6 Summary results for both simulations

Head	Mean coverage	High	Low
Slope coverage, simulation 1	0.9439	0.9532	0.9305
Intercept coverage, simulation 1	0.9478	0.9547	0.9360
Slope coverage, simulation 2	0.9484	0.9528	0.9444
Intercept coverage, simulation 2	0.9500	0.9550	0.9465

An interesting discovery was also made. Namely, the percent coverage for slope is highly sensitive to the precision limit of the input value: When P_x is an order of magnitude greater than P_y, and a large hysteresis effect is present, the slope percent coverage drops significantly. This implies that, in this limited case, one should probably include an elemental uncertainty contribution from the hysteresis if P_x cannot be improved.

Uncertainty Estimates and Data Reporting

The most general form of the propagation equation (ignoring correlated precision uncertainties, which are relatively rare) for the uncertainty in average thrust is given in Eq. (23). This equation accounts for precision uncertainty, bias uncertainty, and correlated bias uncertainty. Thus, to complete the uncertainty. analysis, the elemental uncertainty limits must be estimated.

$$U_{\bar{T}}^2 = \sum_{i=1}^{N}\left(\frac{\partial \bar{T}}{\partial X_i}\right)^2 P_{X_i}^2 + \sum_{i=1}^{N}\left(\frac{\partial \bar{T}}{\partial Y_i}\right)^2 P_{Y_i}^2 + \sum_{i=1}^{n+1}\left(\frac{\partial \bar{T}}{\partial T_i}\right)^2 P_{T_i}^2 + \sum_{i=1}^{N}\left(\frac{\partial \bar{T}}{\partial X_i}\right)^2 B_{X_i}^2 + 2\sum_{i=1}^{N-1}\sum_{k=i}^{N}\left(\frac{\partial \bar{T}}{\partial X_i}\right)\left(\frac{\partial \bar{T}}{\partial X_k}\right) B_{X_i X_k} + \sum_{i=1}^{N}\left(\frac{\partial \bar{T}}{\partial Y_i}\right)^2 B_{Y_i}^2 + 2\sum_{i=1}^{N-1}\sum_{k=i}^{N}\left(\frac{\partial \bar{T}}{\partial Y_i}\right)\left(\frac{\partial \bar{T}}{\partial Y_k}\right) B_{Y_i Y_k} + \sum_{i=1}^{n+1}\left(\frac{\partial \bar{T}}{\partial T_i}\right)^2 B_{T_i}^2 + 2\sum_{i=1}^{n}\sum_{k=i}^{n+1}\left(\frac{\partial \bar{T}}{\partial T_i}\right)\left(\frac{\partial \bar{T}}{\partial T_k}\right) B_{T_i T_k} + 2\sum_{i=1}^{n+1}\sum_{k=i}^{N}\left(\frac{\partial \bar{T}}{\partial T_i}\right)\left(\frac{\partial \bar{T}}{\partial X_k}\right) B_{T_i X_k} + 2\sum_{i=1}^{n+1}\sum_{k=i}^{N}\left(\frac{\partial \bar{T}}{\partial T_i}\right)\left(\frac{\partial \bar{T}}{\partial Y_k}\right) B_{T_i Y_k} + 2\sum_{i=1}^{N}\sum_{k=i}^{N}\left(\frac{\partial \bar{T}}{\partial X_i}\right)\left(\frac{\partial \bar{T}}{\partial Y_k}\right) B_{X_i Y_k} \tag{23}$$

The two load cells used at TS 500 are rated at 50,000 lbf and use strain gauges mounted in a Wheatstone bridge configuration. When a load is applied, the resistance in (at least) one arm of the bridge changes, whereas the input (or excitation) voltage remains constant. This results in an output voltage change that is recorded and converted to pounds-force. The relationship between the output voltage and the applied load is linear, but can be changed by using different gauge factors and zero balance settings (J. Wiley, private communications, 1998–1999).

This linear relationship is what is verified at the calibration facility, and it is highly repeatable. Nevertheless, there will always be some bias in the calibration, determined by the limits of the calibration standard used. Therefore, these load cells, calibrated at the same facility against the same standard, have a systematic uncertainty estimated at 0.5% of FS, or 250 lbf, and these bias uncertainties will be assumed to be fully correlated (J. Elmore, private communication, 1997).

Recall that Fig. 6 shows the calibration data for a subscale test in support of the HPDP. The hysteresis in the calibration curve makes it clear that the motor was not aligned properly. However, what is not clear is how far out of alignment the motor may have been, which represents an experimental uncertainty. This type of bias represents a common, but often overlooked, class of experimental uncertainty called conceptual bias. That is, what occurs experimentally differs from what has been assumed to occur.[5] In this case, the calibration hysteresis shows that the motor is misaligned, violating the assumption that the thrust vector and the TMS centerline are coaxial. Because there are no data to help define what hysteresis results from a given misalignment, this misalignment was arbitrarily (and

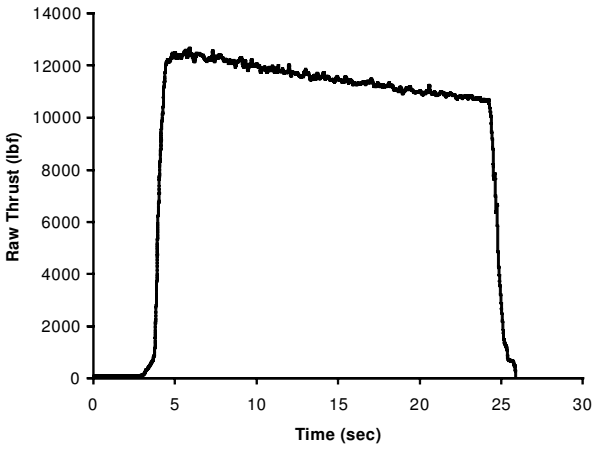

Fig. 10 Raw thrust data.

conservatively)estimated to be 3 in. Then, the bias contribution was then calculated as the sine of the angle formed by the misaligned motor, or approximately 1% of the reading.

Now, a random uncertainty estimate is needed for both load cells, which simply represents the repeatability of multiple observations of the same condition. A sample of these data exist because the data-acquisition system is started before calibration load cycles actually begin, meaning that multiple readings of the zero-load magnitudes on each load cell are recorded. Therefore, the load cell elemental random uncertainty was estimated[5] as two times the sample standard deviation of the mean for the pretest load cell data using Eq. (9), repeated hereafter for convenience. The result was 0.4 lbf for the thrust measurement load cell and 0.5 lbf for the calibration load cell:

$$S_r = \left[\frac{1}{N-1}\sum_{i=1}^{N}(r_i - \bar{r})^2\right]^{\frac{1}{2}} \tag{9}$$

Figure 10, the raw thrust data for the test, helps identify another random uncertainty component: the unsteadiness of the combustion process itself.

This, again, is an instance where the precision limit could be estimated by two times the sample standard deviation of the mean, but, because of nozzle throat erosion and declining fuel flow rate, the thrust data show a steady downward trend. The problem with using the deviation from a single averaged value is that there is a question of what average is used. It seems unlikely that simply using the single-valued time-averaged thrust for $\bar{r}$ would be useful because there is an actual downward trend. A proper estimate must take the trend into account, which indicates that some form of moving average should be used. One simple method would be to fit a first-order, least-squares line to the mainstage thrust, which would effectively separate the trend from the combustion "noise." Then one would be free to calculate the standard error of regression using Eq. (24). When done for the data shown here, that random uncertainty component is 90 lbf.

$$S_{\text{regression}} = \left[\frac{\sum_{i=1}^{N}(r_i - mX_i - c)^2}{N-2}\right]^{\frac{1}{2}} \tag{24}$$

Another situation encountered at TS 500 was that the feed system tare changes at some point during or after the test. Just before the test (as seen in Fig. 10), the zero-thrust load cell reading is approximately 85 lbf, whereas following the test, it is approximately −85 lbf. The cause is not clear, but somehow the strain on the load cell has changed. This has been a long-recognized problem, and it was addressed in the ICRPG practices manual by the suggestion to run a postfire calibration test.[2] However, it was never clear what one was to do with the postfire calibration data, only that "corrective action should be taken immediately" if there was a discrepancy between the two tare measurements.[2]

Table 7 Elemental uncertainty components

Elemental uncertainty component	Calibration load cell, lbf	Thrust load cell
Bias due to laboratory calibration	250	250 lbf
Bias due to misalignment	——	1% of reading
Bias due to zero offset difference	——	85 lbf
Precision due to laboratory calibration	0.5	0.4 lbf
Precision due to unsteady combustion process	——	90 lbf

Table 8 Results of average thrust-uncertainty analysis

Parameter	Value, lbf
Average delivered thrust	12,930
Uncertainty in average delivered thrust	315
Range of delivered thrust	11,685–14,175

The ICRPG uncertainty estimate handbook offered no help because it suggested that the tare history of a given stand should be recorded and that the distribution of those tares should be used to calculate an elemental precision uncertainty.[3] There is a critical difference, however, between the intended use for the ICRPG uncertainty handbook: The estimate outlined is the uncertainty in thrust for a large number of engines taken in a large number of different stands.[3] The analysis in this paper applies only to the average thrust of a single test in a single stand, and so the method in the ICRPG handbook does not apply. It is unsettling, however, that no explanation was given of what corrective action should be taken when there is a distinct difference between pre- and posttest tares in any single engine or motor installation. Therefore, one method to account for the uncertainty resulting from a changing system tare will be given in light of a discussion of the particular load cells at TS 500.

Two ways of changing how a load cell reading can be altered (and, hence, how field calibrations are made) requires changing the zero balance and the gauge factor. In simple terms, the gauge factor controls the slope of output voltage to excitation voltage and a zero balance adjusts the intercept of that input/output curve. These two controls are independent, meaning that one can change the zero-balance setting without disturbing the slope of the input/output curve (J. Wiley, private communications, 1998–1999).

The practical application of this is that if a nonzero zero-load reading (or zero offset) is consistent throughout a test, it is easily corrected in the raw thrust data, given the arguments of the preceding paragraph. One simply subtracts the system tare from the raw thrust data, which is the method suggested by the ICRPG.[3]

It is only when zero offset changes during a test that it contributes an elemental uncertainty to the thrust data, because it is the difference in zero-load readings that causes one not to know exactly which bias to remove from the data. Thus, one may calculate the two offsets (the prehot-fire and posthot-fire zero thrust readings) and adjust the raw data by the average of those two offsets so that the raw thrust data are centered about the x axis. The elemental systematic uncertainty is then estimated by one-half of the difference in offsets. When this procedure was used for this test, the prefire zero thrust tare was 85 lbf, and the postfire tare was −85 lbf. Therefore, that additional elemental systematic error was estimated as 85 lbf.

In summary, Table 7 shows all of the elemental uncertainty components, and Table 8 summarizes the delivered thrust, its uncertainty, and its range. Because the alternate load path due to the LOX feed system was accounted for, and because the calibration hysteresis does not significantly affect the uncertainty in the slope, the overall uncertainty in average delivered thrust is mostly contained in the bias uncertainty estimate in the thrust measurement load cell. The next significant contributors are the bias due to the system tare change and the precision uncertainty associated with combustion noise.

Conclusions

Because thrust is often measured with a simple strain-gauge-based device, it is easy to assume that the process of measuring it is as simple as its measurement device. The work described herein

shows that thrust measurement is easy in theory, but can be difficult in practice. Only with a thorough understanding of the particular test stand and test article interaction can thrust be measured with a high confidence level. The six major conclusions from this effort are listed hereafter:

1) Hysteresis at TS 500 is caused by the friction resulting from poor motor and TMS alignment.

2) Hysteresis at TS 500 was eliminated through proper, independent motor and TMS alignment.

3) Experimental data were presented that distinctly show the interaction between the state of the LOX feed system and the TMS, implying that the feed system must be in the hot-fire test conditions during calibration.

4) Monte Carlo simulations showed that uncertainty in slope and intercept for a regression was unaffected by data that exhibited even high levels of hysteresis. The exception to this rule was in instances where the input variable's random uncertainty was an order of magnitude higher than that of the output variable's random uncertainty. The implication is that a term for hysteresis need not be included in a detailed uncertainty estimate for average thrust.

5) The cause of hysteresis, namely, motor and, hence, thrust vector misalignment, however, must be accounted for in that uncertainty analysis.

6) The major contributor to average thrust uncertainty at TS 500 is the systematic (bias) uncertainty associated with the thrust measurement load cell.

References

[1]Runyan, R. B., Miller, J. T., and Rynd, J. P., Jr., "ETF Thrust Stand Systems—Description, Calibration, and Operation," AD-B160-766, Dec. 1991.

[2]*Handbook of Recommended Practices for Measurement of Liquid Propellant Rocket Engine Parameters*, Chemical Propulsion Information Agency, CPIA 179, 1969.

[3]*ICRPG Handbook for Estimating the Uncertainty in Measurements Made with Liquid Propellant Rocket Engine Systems*, Chemical Propulsion Information Agency, CPIA 180, 1969.

[4]Coleman, H. W., and Steele, G. W., *Experimentation and Uncertainty Analysis for Engineers*, 2nd ed., Wiley, New York, 1999.

[5]Brown, K. K., Coleman, H. W., and Steele, W. G., "A Methodology for Determining Experimental Uncertainties in Regressions," *Journal of Fluids Engineering*, Vol. 120, No. 3, 1998, pp. 445–456.

[6]Atkinson, K., *Elementary Numerical Analysis*, 2nd ed., Wiley, New York, 1985.